Biomedical Optics EXPRESS

Epidural catheter with integrated light guides for spectroscopic tissue characterization

R. P. Soto-Astorga,[1,*] S. West,[2] S. Putnis,[3] J. C. Hebden,[1] and A. E. Desjardins[1]

[1] *Department of Medical Physics and Bioengineering, University College London, London, UK*
[2] *Department of Anaesthesia, University College Hospital, London, UK*
[3] *Department of Orthopaedics, University College Hospital, London, UK*
[*] *rocio.astorga.10@ucl.ac.uk*

Abstract: Epidural catheters are used to deliver anesthetics and opioids for managing pain in many clinical scenarios. Currently, epidural catheter insertion is performed without information about the tissues that are directly ahead of the catheter. As a result, the catheter can be incorrectly positioned within a blood vessel, which can cause toxicity. Recent studies have shown that optical reflectance spectroscopy could be beneficial for guiding needles that are used to insert catheters. In this study, we investigate the whether this technique could benefit the placement of catheters within the epidural space. We present a novel optical epidural catheter with integrated polymer light guides that allows for optical spectra to be acquired from tissues at the distal tip. To obtain an initial indication of the information that could be obtained, reflectance values and photon penetration depth were estimated using Monte Carlo simulations, and optical reflectance spectra were acquired during a laminectomy of a swine *ex vivo*. Large differences between the spectra acquired from epidural adipose tissue and from venous blood were observed. The optical catheter has the potential to provide real-time detection of intravascular catheter placement that could reduce the risk of complications.

OCIS codes: (170.6510) Spectroscopy, tissue diagnostics; (170.3890) Medical optics instrumentation.

References and links

1. M. A. Reina, A. López García, J. A. de Andrés, F. Sellers, M. Arrizabalaga, and M. J. Mora, "Variation in the thickness of the dural sac," Rev. Esp. Anestesiol. Reanim. **46**(8), 344–349 (1999).
2. M. A. Reina, P. Pulido, J. Castedo, M. C. Villanueva, A. López, and R. G. Sola, "Characteristics and distribution of normal human epidural fat," Rev. Esp. Anestesiol. Reanim. **53**(6), 363–372 (2006).
3. J. Abbas, K. Hamoud, Y. M. Masharawi, H. May, O. Hay, B. Medlej, N. Peled, and I. Hershkovitz, "Ligamentum flavum thickness in normal and stenotic lumbar spines," Spine **35**(12), 1225–1230 (2010).
4. J. Guay, "The epidural test dose: A review," Anesth. Analg. **102**(3), 921–929 (2006).
5. T. Fivez, S. Deblonde, and M. Van de Velde, "Late intravascular migration of a previously well functioning labour epidural catheter," Eur. J. Anaesthesiol. **27**(7), 634–636 (2010).
6. S. M. Burns, C. M. Cowa, P. M. Barclay, and R. G. Wilkes, "Intrapartum epidural catheter migration: A comparative study of three dressing applications," Br. J. Anaesth. **86**(4), 565–567 (2001).
7. C. K. Ting, M. Y. Tsou, P. T. Chen, K. Y. Chang, M. S. Mandell, K. H. Chan, and Y. Chang, "A new technique to assist epidural needle placement: Fiberoptic-guided insertion using two wavelengths," Anesthesiology **112**(5), 1128–1135 (2010).
8. J. P. Rathmell, A. E. Desjardins, M. van der Voort, B. H. W. Hendriks, R. Nachabe, S. Roggeveen, D. Babic, M. Söderman, M. Brynolf, and B. Holmström, "Identification of the epidural space with optical spectroscopy: An in vivo swine study," Anesthesiology **113**(6), 1406–1418 (2010).
9. A. E. Desjardins, B. H. W. Hendriks, M. van der Voort, R. Nachabé, W. Bierhoff, G. Braun, D. Babic, J. P. Rathmell, S. Holmin, M. Söderman, and B. Holmström, "Epidural needle with embedded optical fibers for spectroscopic differentiation of tissue: Ex vivo feasibility study," Biomed. Opt. Express **2**(6), 1452–1461 (2011).
10. S. P. Lin, M. S. Mandell, Y. Chang, P. T. Chen, M. Y. Tsou, K. H. Chan, and C. K. Ting, "Discriminant analysis for anaesthetic decision-making: An intelligent recognition system for epidural needle insertion," Br. J. Anaesth. **108**(2), 302–307 (2012).

#196069 - $15.00 USD Received 26 Aug 2013; accepted 27 Aug 2013; published 24 Oct 2013

11. M. Brynolf, M. Sommer, A. E. Desjardins, M. van der Voort, S. Roggeveen, W. Bierhoff, B. H. W. Hendriks, J. P. Rathmell, A. G. H. Kessels, M. Söderman, and B. Holmström, "Optical detection of the brachial plexus for peripheral nerve blocks: An in vivo swine study," Reg. Anesth. Pain Med. **36**(4), 350–357 (2011).
12. A. Balthasar, A. E. Desjardins, M. van der Voort, G. W. Lucassen, S. Roggeveen, K. Wang, W. Bierhoff, A. G. H. Kessels, M. van Kleef, and M. Sommer, "Optical detection of peripheral nerves: An in vivo human study," Reg. Anesth. Pain Med. **37**(3), 277–282 (2012).
13. A. Balthasar, A. E. Desjardins, M. van der Voort, G. W. Lucassen, S. Roggeveen, K. Wang, W. Bierhoff, A. G. H. Kessels, M. Sommer, and M. van Kleef, "Optical Detection of Vascular Penetration During Nerve Blocks: An In Vivo Human Study," Reg. Anesth. Pain Med. **37**(1), 3–7 (2012).
14. J. Zubia and J. Arrue, "Plastic optical fibers: An introduction to their technological processes and applications," Opt. Fiber Technol. **7**(2), 101–140 (2001).
15. S. A. Prahl, M. Keijzer, S. L. Jacques, and A. J. Welch, "A Monte Carlo model of light propagation in tissue," SPIE Institute Series. **IS5**, 102–111 (1989).
16. M. Friebel, A. Roggan, G. Müller, and M. Meinke, "Determination of optical properties of human blood in the spectral range 250 to 1100 nm using Monte Carlo simulations with hematocrit-dependent effective scattering phase functions," J. Biomed. Opt. **11**(3), 034021 (2006).
17. A. N. Bashkatov, E. A. Genina, V. I. Kochubey, and V. V. Tuchin, "Optical properties of human skin, subcutaneous and mucous tissues in the wavelength range from 400 to 2000 nm," J. Phys. D Appl. Phys. **38**(15), 2543–2555 (2005).
18. R. L. P. van Veen, H. J. C. M. Sterenborg, A. Pifferi, A. Torricelli, and R. Cubeddu, "Determination of VIS-NIR absorption coefficients of mammalian fat, with time and spatially resolved diffuse reflectance and transmission spectroscopy," OSA Annual BIOMED Topical Meeting (2004)
19. S. Prahl, "Optical Absorption of Hemoglobin". *http://omlc.ogi.edu/spectra/hemoglobin*
20. D. Arifler, C. MacAulay, M. Follen, and R. Richards-Kortum, "Spatially resolved reflectance spectroscopy for diagnosis of cervical precancer: Monte Carlo modeling and comparison to clinical measurements," J. Biomed. Opt. **11**(6), 064027 (2006).
21. U. Utzinger and R. R. Richards-Kortum, "Fiber optic probes for biomedical optical spectroscopy," J. Biomed. Opt. **8**(1), 121–147 (2003).
22. M. Meinke, G. Müller, J. Helfmann, and M. Friebel, "Optical properties of platelets and blood plasma and their influence on the optical behavior of whole blood in the visible to near infrared wavelength range," J. Biomed. Opt. **12**(1), 014024 (2007).
23. W. White, "Perfluorinated Graded Index Plastic Optical Fiber GigaPOF®". *http://www.chromisfiber.com/pdf/OFC2010Wwhite1105.pdf*

1. Introduction

Epidural anesthesia and analgesia involves mitigating pain with injections into the epidural space. The epidural space is located in the outermost region of the spinal canal, posterior to the dura mater that encloses cerebrospinal fluid and anterior to another tissue layer called the ligamentum flavum. Two prominent constituents of the epidural space are loose adipose tissue and a network of thin-walled interconnected blood vessels called a venous plexus. An injection of local anesthetics and/or opiods into the epidural space can be performed either as a continuous flow through a catheter, or as a single bolus with an injection through a needle. The epidural space is known as a "potential space" since the space is created by an injection. A catheter is typically inserted into the epidural space through a Tuohy needle. With the Tuohy needle in place, the catheter is inserted through the cannula beyond its tip, the needle is withdrawn, and the catheter is left in place (Fig. 1).

#196069 - $15.00 USD Received 26 Aug 2013; accepted 27 Aug 2013; published 24 Oct 2013

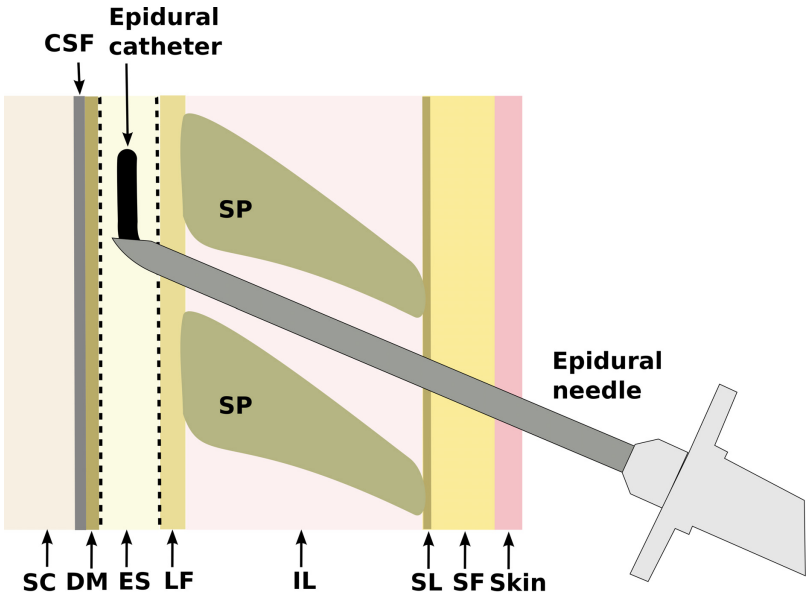

Fig. 1. Simplified schematic of tissue structures in the vicinity of a needle/catheter insertion into the epidural space. SF: subcutaneous fat; SL: supraspinous ligament; IL: interspinous ligament; SP: spinous process; LF: ligamentum flavum; ES: epidural space; DM: dura mater CSF: cerebrospinal fluid; SC: spinal cord. Typical thicknesses of the dura mater, the epidural fat, and the ligamentum flavum are 0.3 mm, 6-13 mm, and 1.4 - 4.7 mm, respectively [1–3].

In many clinical contexts, needles and catheter insertions into the epidural space are performed without image guidance, and therefore there is a significant risk that they are inserted into vascular structures. Intravascular injections can cause toxicity to the nervous and cardiovascular systems that can, if undetected, result in complications such as convulsions, hypoventilation, arrhythmias, hypotension, tachycardia, and cardiac arrest. Current methods for detecting intravascular injections, which include aspirations and test doses with epinephrine, are not completely effective [4]. Moreover, even if epidural catheters are correctly positioned, their tips can migrate into blood vessels due to patient motion [5, 6]. In women, there is an increase in the size of the venous plexus during pregnancy, which may elevate the risk of intravascular catheter tip placement.

Recently, several studies [7–10] have investigated the use of optical reflectance spectroscopy to guide the placement of needles into the epidural space. With this technique, integrated optical fibers deliver light to tissue at the distal end of the needle and receive a portion of the reflected light. In the visible wavelength range, prominent light absorbers include oxy- and deoxy-hemoglobin; in the near-infrared, they include lipid, and water. The optical spectra of the received light can be processed to highlight differences in the concentrations of these chromophores and differences in the wavelength-dependence of optical scattering. As such, they can be used to perform tissue classification. With *in vivo* porcine and human studies, the potential to directly detect incorrect placement of needles into vascular structures was also demonstrated [11–13]. The use of optical reflectance spectroscopy to monitor the placement of epidural catheters has remained, to the authors' knowledge, unexplored.

In this study, we present a novel optical epidural catheter with integrated light guides. These light guides allowed for light to be delivered and received at the catheter tip. Reflectance values and photon penetration depth were estimated using Monte Carlo simulations, and spectra were acquired during a post-mortem laminectomy of a swine.

#196069 - $15.00 USD Received 26 Aug 2013; accepted 27 Aug 2013; published 24 Oct 2013

2. Materials and methods

2.1 Optical catheter

The optical epidural catheter had an outer diameter of 842 μm, an inner diameter of 447 μm, and a length of 1 m. These dimensions were consistent with those of commercial epidural catheters. Four light guides were integrated into the catheter wall. Each light guide had an outer diameter of 125 μm and a core diameter of 109 μm. The light guides were arranged symmetrically (Fig. 2).

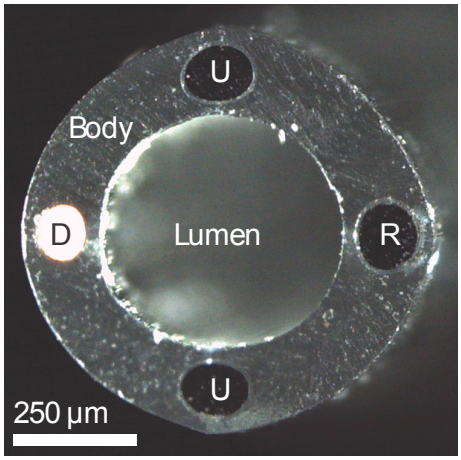

Fig. 2. Distal end of the optical catheter. D: delivery light guide; R: receive light guide; U: unused light guide.

The catheter was developed with a polymer extrusion process (Paradigm Optics, Vancouver, WA) that included polystyrene for the body, polymethyl methacrylate (PMMA) for the light guide core, and THV 500G (a polymer of tetrafluoroethylene, hexafluoropropylene and vinylidene fluoride) for the light guide cladding. While the optical light guides had a transparent visual appearance, prominent absorption in the near-infrared in the vicinity of 700 nm, 900 nm, and 1000 nm were apparent in the transmission spectrum (Fig. 3). These absorption peaks are consistent with previous studies [14]. The transmission spectrum was measured using one of the light guides from an optical catheter (1 m length) and a silica/doped-silica core/cladding fiber (AFS105/125, Thorlabs; 1 m length) as a reference.

#196069 - $15.00 USD Received 26 Aug 2013; accepted 27 Aug 2013; published 24 Oct 2013

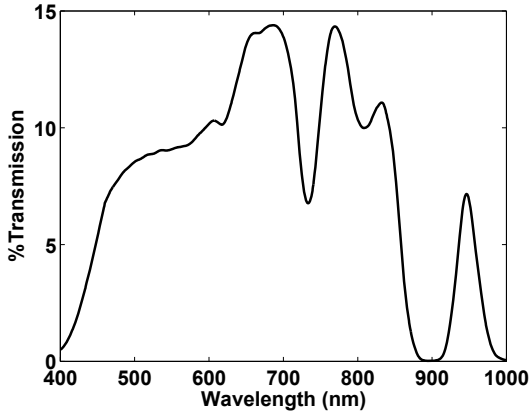

Fig. 3. Transmission of the polymer guides embedded in the catheter. Prominent absorption peaks can be seen at wavelengths of 730, 900 and 1000 nm.

At the proximal end of the catheter, 20 cm of the light guides were exposed by dissolving the polystyrene body with cyclohexane. Two of the light guides on opposite sides of the catheter were connectorized. When exposed, the light guides had diameters slightly larger than 125 μm (which probably occurred due to incomplete dissolution of the surrounding polystyrene), so a diameter of 230 μm was chosen for the inner lumens of the SMA connectors. The other two light guides were not used in this study. One connectorized light guide delivered broadband light to tissue from a tungsten-halogen source (HL-2000, Ocean Optics). The other received reflected light from tissue and delivered it to a spectrometer with a silicon detector array (MayaPro, Ocean Optics). The system schematic is shown in Fig. 4.

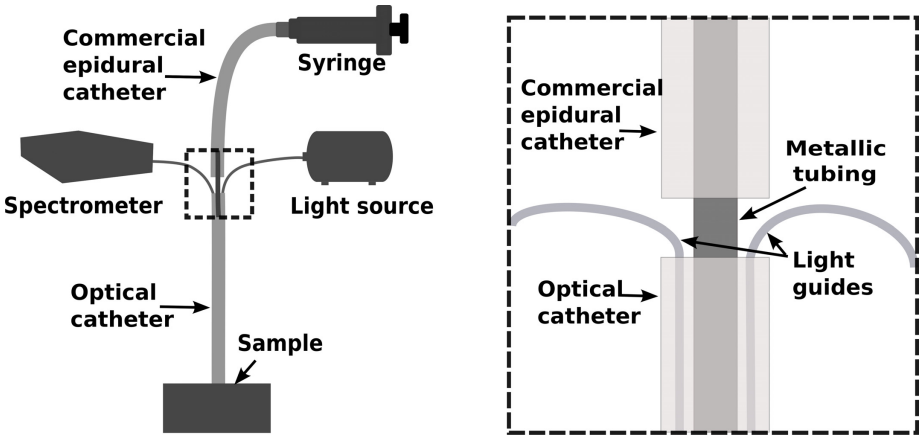

Fig. 4. System schematic. The two connectorized light guides are connected to the source and detector, respectively. At the proximal end, the optical catheter is coupled to a commercial epidural catheter with metallic tubing to allow for fluid to be injected into the lumen.

The spectrometer was interrogated with a custom software written in LabVIEW (National Instruments, Austin, TX), which provided a real-time display of the raw and processed spectra. The processing of the spectra acquired from tissue, $S_{\text{tissue}}(\lambda)$, included two steps: background correction and white-balancing. Background correction involved subtraction of a dark current spectrum, $S_{\text{dark}}(\lambda)$, which was obtained with the light source turned off. White balancing involved division by a background-corrected reference spectrum, $S_{\text{ref}}(\lambda)$, which was acquired from a diffuse reference standard (SRM-99, Labsphere, North Sutton, NH) with

#196069 - $15.00 USD Received 26 Aug 2013; accepted 27 Aug 2013; published 24 Oct 2013

the catheter tip positioned 1 mm above the surface. These processing steps, which generated a calibrated tissue spectrum $S(\lambda)$, are summarized by Eq. (1):

$$S(\lambda) = \frac{S_{\text{tissue}}(\lambda) - S_{\text{dark}}(\lambda)}{S_{\text{ref}}(\lambda) - S_{\text{dark}}(\lambda)} \quad (1)$$

To facilitate interpretation of the calibrated spectra, two parameters were calculated. The first parameter, *H*, was calculated from the values of the calibrated spectrum at two isobestic points of the hemoglobin absorption spectrum, λ_1 = 796 nm and λ_2 = 545 nm, as shown in Eq. (2):

$$H = \frac{S(\lambda_1) - S(\lambda_2)}{S(\lambda_1)} \quad (2)$$

The hemoglobin parameter, *H*, was previously defined in a study that investigated the detection of intravascular penetration events during needle insertions performed for nerve blocks in human patients [12]. This parameter, which involves two wavelengths at isobestic points of the hemoglobin spectrum, is sensitive to hemoglobin content since absorption at one wavelength (λ_2) is much larger than at the other wavelength (λ_1). The normalizing term $S(\lambda_1)$ is used to compensate for any changes in overall intensity. An increase in the hemoglobin parameter is consistent with an increase in the hemoglobin content of tissue from which the spectrum derived, provided that optical scattering is constant. The second parameter was the intensity *I*, which was calculated as average value of a calibrated spectrum over the wavelength range of 450 nm to 850 nm.

Access to the catheter lumen for fluid injections was provided by coupling the proximal end of the catheter to a commercial catheter. This coupling was performed with a metal tube that was obtained from a 27-gauge needle (outer/inner diameters: 413/210 μm) with a total length of 15 mm. The ends of this metal tube were inserted into the lumens of the optical and commercial catheters to distances of 7 mm and secured with epoxy (F120, Thorlabs).

2.2 Monte Carlo analysis

Monte Carlo simulations were performed with custom software that was based on the algorithm described by Prahl et al. [15], with the angular dependence of scattering modeled with the Henyey-Greenstein phase function. In each simulation, the source-detector separation (as measure from the center of the delivery light guide to the center of the retrieving light guide) was 644 μm to match the geometry of the optical catheter (Fig. 2). The position from which photons entered tissue was sampled from a probability distribution derived from the spatial dimensions of the light guide core and the numerical aperture (NA) of the light guide. With the refractive indices of THV and PMMA taken to be 1.35 and 1.49, respectively, the NA of the light guide was 0.63. The custom software was written in C and executed within Matlab (Mathworks, Natick, MA) to facilitate post-processing and display.

The optical properties of tissue were chosen to simulate photon propagation for two tissue types: blood with 80% oxygenation, and adipose tissue. For each tissue type, simulations were performed for 6 wavelengths that spanned the wavelength range of 450 nm to 850 nm. At each wavelength, 6 simulations were performed, with 1.5×10^6 photons used in the simulation. The scattering properties of blood and adipose tissue were obtained from Friebel et al. [16] and Bashkatov et al. [17], respectively. The absorption coefficients of these tissues were obtained from tabulated data [18, 19].

2.3 Ex-vivo laminectomy

A laminectomy at a lumbar level of a spine was performed that ultimately exposed the spinal cord. This laminectomy was performed at Northwick Park Institute for Medical Research (NPIMR). The intact adult swine (Large White; female; 50 kg) was received approximately

#196069 - $15.00 USD Received 26 Aug 2013; accepted 27 Aug 2013; published 24 Oct 2013

15 minutes after sacrifice, and the laminectomy was conducted within a time period of 2 hours. The swine had been used in the context of an *in vivo* experiment by another research group that involved a superficial skin experiment. Therefore, as verified by the NPIMR, additional ethics approval was not required for the experiments conducted in this study. The previous experiment did not affect the lumbar region of the spine and did not involve the use of optical contrast agents.

The laminectomy was performed in stages. At each stage, a new tissue layer was revealed, and the catheter was manually positioned with its distal tip perpendicular to the tissue surface (Fig. 5). Care was taken not to exert pressure on the tissue with the catheter. Spectra were obtained from the surfaces of tissue types commonly encountered by the distal tip of an epidural catheter: ligamentum flavum, epidural fat, and dura mater. Additionally, spectra were obtained from a 5 mL sample of venous blood extracted from the epidural venous plexus that was placed in a test tube (diameter: 1 cm); the catheter was positioned in the center of the sample. For each tissue type, 20 spectra were acquired with a 1 second integration time per spectrum.

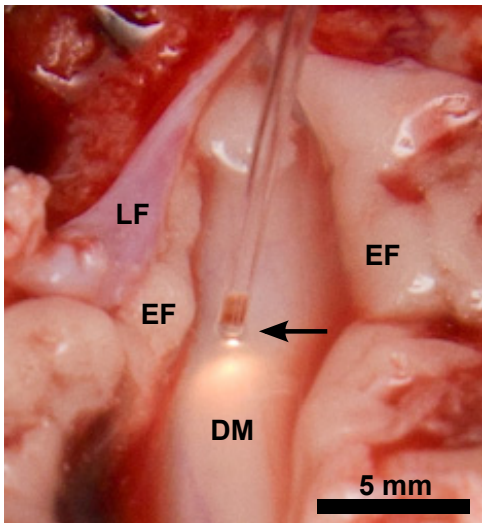

Fig. 5. The region around the spinal cord showing the tip of the optical catheter (arrow) on the surface of the dura mater (DM). Adjacent to the DM were the epidural fat (EF) and the ligamentum flavum (LF).

3. Results

3.1 Monte Carlo simulations

According to Monte Carlo simulations, the relative intensities of light obtained at two isobestic points of the hemoglobin absorption spectrum, 545 nm and 797 nm, varied between adipose tissue and blood. As described in the Introduction section, these tissues are clinically significant: the target location for epidural catheters is the adipose tissue within the epidural space, and complications can arise when epidural catheters enter veins and anaesthesia or opioids are inadvertently introduced into the blood stream. With adipose tissue, the intensity of light at 545 nm was 125% of the intensity of light at 797 nm; with venous blood, the former was 4% of the latter. The hemoglobin values calculated from these relative intensities were $H_{\text{fat}} = -0.2580 \pm 0.0029$, and $H_{\text{blood}} = 0.9596 \pm 0.0003$, respectively (Table 1). The average depth reached by the detected photons was greater overall for adipose tissue than for blood. For adipose tissue, it varied from 0.90 mm to 1.03 mm for the wavelengths used in the simulations. For blood, it varied from 0.06 mm at 545 nm (where hemoglobin absorption is prominent), to 0.51 mm at 797 nm (where it is less prominent).

#196069 - $15.00 USD Received 26 Aug 2013; accepted 27 Aug 2013; published 24 Oct 2013

Table 1. Tissue Reflectivity and Average Maximum Depth for Adipose Tissue and Venous Blood Calculated with Monte Carlo Simulations

		Simulation Parameters				Calculated Values	
Tissue ype	Wavelength (nm)	μ_a (mm^{-1})	μ_s (mm^{-1})	g	μ_s' (mm^{-1})	Average maximum depth (mm)	Relative reflectance*
Fat	450	0.0064	16.5	0.9	1.65	0.90 ± 0.66	1.3442 ± 0.0016
	545	**0.0008**	**14.5**	**0.9**	**1.45**	**0.94 ± 0.68**	**1.2580 ± 0.0011**
	650	0.0005	12.8	0.9	1.28	0.98 ± 0.70	1.1365 ± 0.0012
	750	0.0010	11.7	0.9	1.17	1.01 ± 0.71	1.0320 ± 0.0013
	797	**0.0004**	**11.2**	**0.9**	**1.12**	**1.02 ± 0.72**	**1.0000 ± 0.0021**
	850	0.0006	10.7	0.9	1.07	1.03 ± 0.73	0.9550 ± 0.0012
Blood	450	35.4	65	0.95	3.25	0.04 ± 0.01	0.0250 ± 0.0002
	545	**25.3**	**65**	**0.95**	**3.25**	**0.06 ± 0.02**	**0.0357 ± 0.0003**
	650	0.52	75	0.97	2.25	0.49 ± 0.20	0.7868 ± 0.0011
	750	0.35	75	0.97	2.25	0.52 ± 0.23	0.9291 ± 0.0013
	797	**0.4**	**75**	**0.97**	**2.25**	**0.51 ± 0.22**	**0.8829 ± 0.0007**
	850	0.5	75	0.97	2.25	0.49 ± 0.21	0.8053 ± 0.0008

* Reflectance values were calculated by normalizing the number of detected photons at a given wavelength to those at 797 nm.

3.2. Laminectomy

The spectra acquired from tissues during the laminectomy exhibited absorption peaks, which manifested as lower signal intensities within specific wavelength ranges (see Fig. 6). Absorption peaks at wavelengths in the range of 500 nm to 600 nm were consistent with the presence of hemoglobin [19], which included those at 542 nm and 576 nm (oxy-hemoglobin) and 556 nm (deoxy-hemoglobin). Deoxy-hemoglobin absorption peaks at 757 nm [19] were not visually apparent.

Several artifacts in the spectra were apparent. Absorption peaks at 733 nm correspond to the prominent absorption peak of the light guides (Fig. 3) and are consistent with imperfect background subtractions or white-balancing. Negative regions in the spectra acquired from blood are consistent with imperfect background subtractions; for low intensities of reflected light, changes in ambient light in the room affected the spectra.

Pronounced differences in the intensity and hemoglobin parameters obtained from blood and from the other three tissue types were observed. In particular, the mean intensity parameter obtained from blood tissue was 45-fold smaller than that obtained from adipose tissue. The relative similarities between the mean intensity parameters obtained from the ligamentum flavum, dura mater, and epidural fat were consistent with the very similar visual appearances of these three tissues. The mean hemoglobin parameter obtained from adipose tissue was 14-fold smaller than that obtained from blood tissue. The relative similarities of the mean hemoglobin parameters obtained from the other tissues were consistent with their white visual appearances.

#196069 - $15.00 USD Received 26 Aug 2013; accepted 27 Aug 2013; published 24 Oct 2013

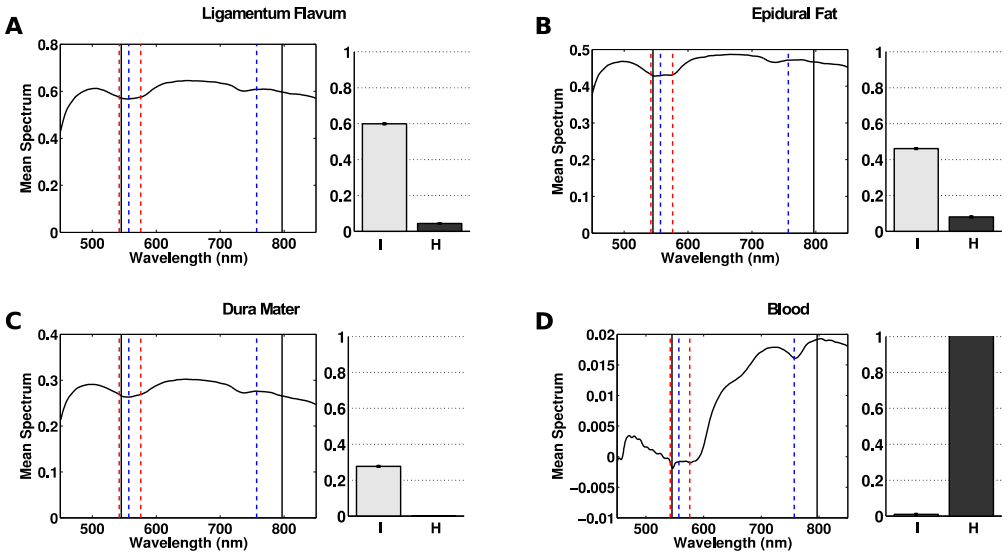

Fig. 6. Mean spectra acquired during the laminectomy from ligamentum flavum (**A**); epidural fat (**B**); dura mater (**C**); blood (**D**). Dashed vertical lines correspond to hemoglobin absorption peaks (red: oxy-hemoglobin; blue: deoxy-hemoglobin). Solid vertical lines correspond to the isobestic points of the hemoglobin absorption spectrum that were used to calculate the hemoglobin parameter. To the right of each spectrum: the corresponding mean intensity (I) and hemoglobin (H) parameters and their standard deviations.

4. Discussion

This catheter was, to the authors' knowledge, the first epidural catheter with integrated light guides. With dimensions consistent with commercially-available catheters, it allowed for the acquisition of optical reflectance spectra from tissue at the distal tip in real-time, and for injections of fluid through its lumen.

The measurements acquired from the epidural region of the swine with the optical catheter during the laminectomy demonstrated that there were prominent differences in the optical reflectance spectra acquired from blood and from adjacent tissues. This finding is clinically significant, as it highlights the potential of optical reflectance spectroscopy to provide catheter guidance and to detect intravascular catheter tip placement in particular.

The catheter used in this study had four light guides but only two were used in this pilot study. Reflectance measurements with different source-detector distances could be performed if additional light guides were used, which would have the potential advantage of performing spectroscopic sensing at different depths in tissue [20, 21]. For the geometry of the light guides, the source-detector separation was 644 μm. The resulting average maximum depth in the fat and blood tissue simulations was consistent with those obtained by Arifler et al. [20].

The hemoglobin and intensity parameters facilitated comparisons between spectra. An important benefit of these parameters is that they can be related in a straightforward manner to visual features in the spectra. A limitation is that they are not directly related to chromophore concentrations or to morphological features of tissue. Indeed, they can be confounded by the presence of additional tissue chromophores such as beta-carotene, and by variations in the wavelength dependence of optical scattering. To estimate the concentrations of oxy- and deoxy-hemoglobin in tissue, it may be important to account for multiple factors such as the aggregation and flow of erythrocytes, and the concentrations of plasma constituents such as bilirubin and platelets [22].

With measurements limited to one cadaveric specimen, the observed differences in the acquired spectra and the corresponding hemoglobin and intensity parameters provide only an initial indication of the variability of the spectra. Follow-up studies performed in multiple

#196069 - $15.00 USD Received 26 Aug 2013; accepted 27 Aug 2013; published 24 Oct 2013

subjects *in vivo* are required to determine optimal thresholds for the hemoglobin and intensity parameters and to estimate the sensitivity and specificity with which detection can be performed. In an *in vivo* context, several factors could influence the optical reflectance spectra, including tissue heterogeneity, variable amounts of beta-carotene in the epidural fat [2], and variations in the pressure imparted by the catheter on tissues. The volume of saline that is injected by the Tuohy needle as part of the loss-of-resistance test used to detect the epidural space, which may affect the delivery and collection of light at the optical catheter tip, is variable. Follow-up studies are required to determine differences between optical reflectance spectra acquired with the catheter tip within an epidural vein and adjacent to the outer surface.

The materials used for construction of this catheter prototype had several limitations. As a material to construct the catheter body, polystyrene had the advantage that it could readily be removed with cyclohexane to expose the optical light guides. However, its use resulted in a catheter that was more rigid than commercially available ones, and the optical catheter in this study broke for bending radii in the range of 1.5 to 2 cm. These mechanical characteristics are incompatible with clinical practice. Future versions of the catheter could be developed with more flexible materials such as a medical grade polycarbonate such as Zelux GS (David Welker, Paradigm Optics, personal communication). Second, the PMMA light guides had prominent absorption peaks in the visible range and the very low transmission made impractical for wavelengths greater than 1000 nm. Prominent absorption spectra at 1210 nm were previously shown to be relevant for guiding a spinal needle into the epidural space [9] and it is likely that they could be advantageous for catheter guidance as well. The limitations of PMMA could potentially be overcome with certain perfluorinated plastic optical fibers that allow for transmission at wavelengths up to 1300 nm [23]. Along the translational path, maintaining low fabrication costs will be an important consideration, as catheters are disposable products in current clinical practice.

Modifications to fiber coupling are required make the optical catheter compatible with current clinical practice. Typically, a Tuohy needle is withdrawn over the entire length of the catheter after the catheter has been inserted. This procedure could not be performed if conventional optical fiber connectors are present at proximal ends of the light guides; the connectors are too bulky to fit within the needle. In future versions of the optical catheter, this problem could be solved by performing light coupling into the light guides without optical fiber connectors, using optical side ports in the body of the catheter.

In future versions of the catheter, the distal end will be modified. In typical commercial catheters, fluids are released through multiple holes that extend from the lumen to the side wall, with the distal end face sealed. To allow for optical reflectance measurements to be acquired from the distal end, the holes will need to be positioned carefully to avoid intersections with the light guides. The light guides could be modified so that light is directed to the side wall, perpendicular to the long axis of the catheter, to allow for sensing in the specific regions where fluids are released.

An epidural catheter is usually considered a passive device that is only used to inject fluids. We have demonstrated that optical spectra can be acquired with an active optical component that allows for tissue sensing. The promising results of this study set the stage for real-time detection of serious clinical complications that are currently unaddressed, and they highlight design considerations for future epidural catheters with integrated light guides.

#196069 - $15.00 USD Received 26 Aug 2013; accepted 27 Aug 2013; published 24 Oct 2013